

Attraction and condensation of driven tracers in a narrow channel

Asaf Miron¹, David Mukamel¹ and Harald A Posch²

¹*Department of Physics of Complex Systems, Weizmann Institute of Science, Rehovot 7610001, Israel*

²*Computational Physics Group, Faculty of Physics, University of Vienna, Austria*

Emergent bath-mediated attraction and condensation arise when multiple particles are simultaneously driven through an equilibrated bath under geometric constraints. While such scenarios are observed in a variety of non-equilibrium phenomena, with an abundance of experimental and numerical evidence, little *quantitative* understanding of how these interactions arise is currently available. Here we approach the problem by studying the behavior of two driven "tracer" particles, propagating through a bath in a 1D lattice with excluded-volume interactions. We analytically explore the mechanism responsible for the tracers' emergent interactions and compute the resulting effective attractive potential. This mechanism is then numerically shown to extend to a realistic model of hard driven Brownian discs confined to a narrow 2D channel.

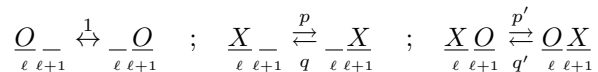
The physics governing the motion of a tracer particle, forcibly driven along a dense medium and confined to a narrow channel, has been extensively explored in recent decades. Besides its immediate relevance to various biological systems [1–5], complex fluids, polymer solutions and glassy dynamics [6–14], this ubiquitous scenario lies at the core of two important technological applications: active microrheology, where microscopic probes are driven along a sample to investigate its spatio-temporal response properties [15–18], and microfluidic devices, where colloids are manipulated through an intricate array of microscopic channels, carefully engineered to perform different tasks [19, 20].

The ubiquity of driven tracer systems has stimulated vigorous theoretical activity, aimed at providing understanding for the collective dynamics induced by a driven tracer in geometrically confined and strongly interacting many-body systems [1, 21–32, 34]. While theoretical efforts have mostly focused on the case of a single driven tracer, the applications noted above typically involve *multiple* driven tracers simultaneously, substantially complicating the picture. Correspondingly, the cooperative behavior of multiple driven tracers has recently attracted considerable attention [35–39]. Extensive numerical studies of multiple tracers in 2D and 3D systems have shown that the surrounding fluid mediates *attractive* interactions between the tracers, leading them to cluster and form a condensate [35, 36]. Studies of 1D lattice models whose single-file dynamics stems from a simple symmetric exclusion process (SSEP), whereby each lattice site may hold one particle at most, have also demonstrated cooperative aspects of the tracer dynamics [37, 38]. In this setting, though, where particles cannot overtake each other, the tracers cannot get too close since the number of bath particles between each pair of tracers is conserved under the dynamics. In a recent numerical study involving a finite density of driven tracers, it was shown that the tracers tend to aggregate and form clusters which, for a sufficiently narrow chan-

nel, could lead to the formation of a plug [39]. Yet, in spite of the vast attention this problem has received, there is still no clear *quantitative* understanding of the mechanism responsible for the bath-mediated attractive interactions between multiple tracers, nor their resulting condensation.

In this Letter we study the mechanism responsible for the attractive interactions arising when multiple tracers are driven through a dense medium inside a narrow channel. To this end, we extend the 1D lattice SSEP model to account for the possibility of particle overtaking which, in the presence of multiple driven tracers, allows an analytical study of their attraction mechanism. Specifically, Our analysis uncovers a regime in which two driven tracers strongly attract one another, forming a robust bound state. Within this regime, we compute the effective potential between two tracers. We trace this entropic attraction back to the inhomogeneous bath density profile generated by the tracers in their respective frames of reference, which acts to restrict their motion and mediates their emergent interactions. With this insight, we construct an effective picture in which the tracers are modeled by independent random walkers whose moving rates are determined by the local density of the surrounding fluid. We compute the resulting attractive potential between the tracers in the steady state, and demonstrate that the fluid's density effectively forces the tracers towards one another, resulting in a bound state. These findings, naively obtained and valid only for our simple lattice model, are argued to serve as a far more general mechanism for attraction and condensation in driven systems. This is corroborated via extensive numerical simulations of a realistic model, reminiscent of the biological systems and technological applications noted above, composed of disk-shaped, hard-core Brownian particles confined to a narrow 2D channel. In particular, qualitatively similar bath-density profiles, as well as emergent tracer attraction and condensation, are clearly observed.

SSEP is a canonical lattice model for interacting many-body systems, describing particles hopping along a 1D lattice with hard-core interactions that prevent them from overtaking one another [40]. Yet, our interest lies in scenarios where overtaking *is* possible, albeit significantly suppressed by geometric constraints. Such conditions were shown to facilitate attraction and condensation when some of the particles are externally driven by a fixed force [35–39]. We extend the standard SSEP dynamics by introducing driven "tracer" particles and allowing overtaking at finite rates. Specifically, we consider a 1D ring of L (even) sites, labeled $\ell = -L/2 + 1, \dots, -1, 0, 1, \dots, L/2$, which are occupied by M tracer particles and N bath particles with mean density $\bar{\rho} = N/(L - M)$. All particles interact via exclusion, whereby each site may hold one particle at most. Bath particles attempt hops to neighboring right and left sites with equal rates 1, whereas the external force biasing the tracers' hopping rates is manifested by their asymmetry, p to the right and q to the left, with $p \neq q$. Particle overtaking is introduced into these dynamics by allowing a tracer to exchange sites with a bath particle occupying its neighboring right and left sites with respective rates p' and q' . This dynamics is conveniently illustrated by



with lattice sites denoted by their respective indices, tracers denoted by X , bath particles denoted by O , holes denoted by vacant sites and the rates of each process are depicted along their corresponding arrows.

This model was first introduced in [1]. Its phase diagram, for the case of a single driven tracer, was characterized by the tracer's stationary velocity and the bath density's profile, as viewed in the tracer's reference frame. By varying the dynamical rates p, q, p', q' and the mean bath density $\bar{\rho}$, two phases were demonstrated: a "localized" phase, where the driven tracer attains a finite velocity and generates a localized deviation of the bath density from $\bar{\rho}$, and an "extended" phase, where the tracer's velocity vanishes as the inverse system size and the bath density profile extends across the entire system. Here we instead consider a number of tracers and show that, in certain regions of the model's parameter space, the tracers strongly attract each other and form a condensate. This is best demonstrated by Fig. 1, which presents a typical trajectory of four tracers in both the lattice model and the 2D channel of hard-core Brownian disks. We hereafter focus on condensation in the model's "localized" phase, noting that a similar analysis and conclusions are valid in the "extended" phase.

To probe the driven tracers' attraction mechanism, it suffices to consider just two of them. The idea is

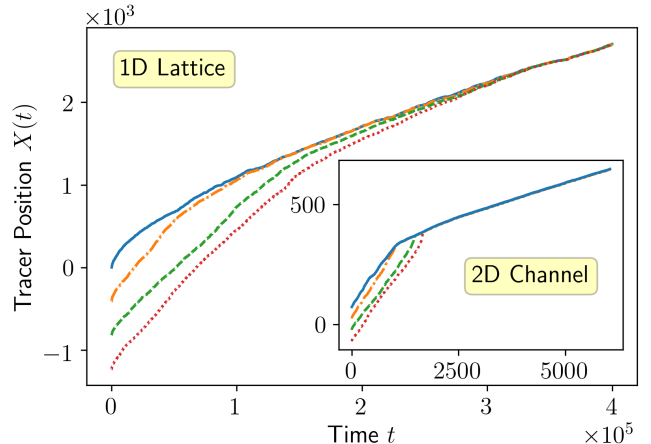


Figure 1. Trajectories of four tracers in a ring of $L = 2048$ sites with a bath density of $\bar{\rho} = 0.2$ and rates $p = 1$ and $q = p' = q' = 0.001$. Inset: Trajectories of four hard-core, Brownian disk tracers driven by a force $F = 16$ through a bath of density $\bar{\rho} = 0.5$ along a 2D narrow channel of width $L_y = 2.1$ and periodic length $L_x = 190$.

to model the tracers as random walkers whose moving rates are determined by the bath density in their vicinity. We use the density profile derived in [1] for a single driven tracer, which remains nearly identical to that arising for two bound driven tracers (see [41]). We then demonstrate that, for strong drive and sufficiently small overtaking rates, the bath density acts to "push" the tracers towards one another. To quantify this effect, we take the thermodynamic limit $L \rightarrow \infty$ and formulate an equation for the distribution P_{n_0, n_1} of the number of holes n_0 and bath particles n_1 between the two tracers. We then solve P_{n_0, n_1} in the long-time limit and derive the stationary distribution $Q(k)$ for the total distance $k = n_0 + n_1$, given by $Q(k) = \sum_{n_0+n_1=k} P_{n_0, n_1}$. Our analysis is concluded upon showing that $Q(k)$ decays exponentially with k , indicating that the tracers effectively interact via a linear attractive potential which results in a bound state.

First, note that n_0 and n_1 are uniquely defined in the $L \rightarrow \infty$ limit: the instantaneous position of the rightmost "tracer 1" sets the location of site $\ell = 0$. The second tracer, called "tracer 2", is then located at site $\ell = -(k + 1)$ (see Fig. 2). We henceforth refer to tracer moves that *reduce* k as "inward" moves, while moves that *increase* k are called "outward" moves. The master equation for P_{n_0, n_1} is then

$$\begin{aligned} \partial_t P_{n_0, n_1} = & (R_+^h \nabla_-^{n_0} + R_-^h \nabla_+^{n_0}) P_{n_0, n_1} \\ & + (R_+^b \nabla_-^{n_1} + R_-^b \nabla_+^{n_1}) P_{n_0, n_1}, \end{aligned} \quad (1)$$

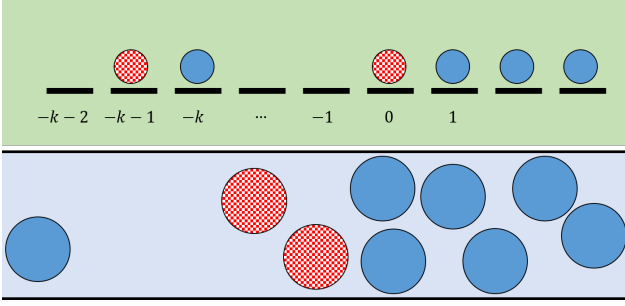


Figure 2. Illustrations of the 1D lattice model (top), explicitly demonstrating the site labeling along the chain, and the 2D channel (bottom). Tracers are depicted by checkered red disks and bath particles by solid blue disks.

where $\nabla_{\pm}^{n_0} P_{n_0, n_1} \equiv P_{n_0 \pm 1, n_1} - P_{n_0, n_1}$ and $\nabla_{\pm}^{n_1} P_{n_0, n_1} \equiv P_{n_0, n_1 \pm 1} - P_{n_0, n_1}$ are the discrete gradient operators. Equation (1) is supplemented with the “boundary” condition $P_{n_0, n_1} = 0$ for $n_0 < 0$ or $n_1 < 0$. The moving rates $R_+^h, R_-^h, R_+^x, R_-^x$ respectively correspond to moves that introduce a hole between the tracers by hopping outwards, remove a hole by hopping inwards, introduce a bath particle by exchanging outwards and remove a bath particle by exchanging inwards.

Due to the model’s exclusion interactions and exchange dynamics, the moving rates $R_{\pm}^{h,x}$ in Eq. (1) naturally depend on the instantaneous bath particle occupation at sites $\ell = \mp 1$ and $\ell = -(k+1) \mp 1$, adjacent to tracers 1 and 2 respectively. As we are interested in the stationary solution of Eq. (1), we employ a “mean field” (MF) approximation to replace the instantaneous site occupations by their stationary average density ρ_{ℓ} . This completes the reduction of the model’s dynamics to that of two biased random walkers whose moving rates are determined by the stationary bath density around them. These rates are given by

$$R_+^h = p(1 - \rho_1) + q(1 - \rho_{-k-2}), \quad R_+^x = p'\rho_1 + q'\rho_{-k-2} \quad (2)$$

$$R_-^h = q(1 - \rho_{-1}) + p(1 - \rho_{-k}), \quad R_-^x = q'\rho_{-1} + p'\rho_{-k} \quad (3)$$

with ρ_n and $(1 - \rho_n)$ replacing the respective instantaneous occupation and vacancy of site n .

With the solid footing provided by Eqs. (1)-(3), we proceed to demonstrate the emergence of a two-tracer bound state. We consider a forward-biased drive $p > q$ with $p \sim \mathcal{O}(1)$ and note the following trivial observation: if the two tracers are initially placed at adjacent sites and no overtaking is allowed, i.e. $p' = q' = 0$, the number of bath particles between the tracers remains 0 at all times. Imagine tracer 1 is initially placed in front of tracer 2. Due to the forward bias, it quickly

advances as far as it can to the right, until it is stopped by exclusion interactions with a stray bath particle. Focusing on the limit $q(1 - \bar{\rho}) \ll 1$, which corresponds to either a strong hopping bias $q \ll 1$ or a large mean bath density $1 - \bar{\rho} \ll 1$, tracer 2 quickly closes any gap that forms between them. In this trivial case the two tracers clearly remain close to one another, leading to condensation in the stationary state. While the existence of a two-tracer bound state is not very surprising under such restrictive single-file settings, its persistence in the presence of *finite* overtaking rates is far from obvious.

Let us keep then the same forward hopping bias $p \sim \mathcal{O}(1) > q$ and $q(1 - \bar{\rho}) \ll 1$ limits and introduce small overtaking rates $p', q' \ll 1$. Determining the tracers’ moving rates, R_{\pm}^h, R_{\pm}^x in Eqs. (2) and (3), requires knowledge of the stationary bath densities near the tracers. If the two tracers do form a bound state, where the typical distance between them is very small, we may think of this bound pair as a single “effective” driven tracer. The density profile ρ_{ℓ} obtained in [1] for a single driven tracer is then also valid for the bound pair, as supported by numerical simulations comparing the profiles in both cases (see [41]). We thus use the results $\rho_1 = \bar{\rho} \frac{p - (1 - \bar{\rho})(q - q')}{p\bar{\rho} + p'(1 - \bar{\rho})}$ and $\rho_{-(k+2)} = \bar{\rho}$ of [1] to determine the outward moving rates R_+^h and R_+^x . To leading order in the small parameters $p', q', q(1 - \bar{\rho})$, Eq. (2) yields

$$R_+^h = 2(1 - \bar{\rho})q - (1 - \bar{\rho})q' + \frac{(1 - \bar{\rho})}{\bar{\rho}}p', \quad (4)$$

$$R_+^x = p' + q'(1 - \bar{\rho}), \quad (5)$$

where $R_+^h, R_+^x \ll 1$. We are then left to determine the inwards moving rates R_-^h, R_-^x .

On time scales smaller than the inverse of R_+^h, R_+^x , the distance between the tracers remains mostly unchanged. The bath particles located between them, which symmetrically attempt hops to both sides with rate 1, quickly relax to a stationary state with a uniform distribution, implying $\rho_{-1} = \rho_{-k} = \frac{n_1}{n_0 + n_1}$ and $1 - \rho_{-1} = 1 - \rho_{-k} = \frac{n_0}{n_0 + n_1}$. The inward moving rates in Eq. (3) thus become

$$R_-^h = (p + q)n_0 / (n_0 + n_1), \quad R_-^x = (p' + q')n_1 / (n_0 + n_1). \quad (6)$$

Equation (1), together with Eqs. (4)-(6), can now be used to determine the stationary distribution P_{n_0, n_1} . Verifying the two-tracer bound state in the *absence* of overtaking provides a welcome consistency check. Substituting $n_1 = p' = q' = 0$ yields $P_{n_0, 0} \propto (R_+^h / (p + q))^{n_0}$. Since $R_+^h / (p + q) \ll 1$, the stationary probability indeed decays exponentially with n_0 .

We are finally ready to tackle the far more interesting case of *finite* exchange rates $p', q' \ll 1$. The leading order solution in small $a \equiv R_+^h/(p+q)$ and $b \equiv R_+^x/(p'+q')$ assumes the form

$$P(n_0, n_1) = A(n_0, n_1) a^{n_0} b^{n_1}, \quad (7)$$

where $a = \frac{1-\bar{\rho}}{p+q} \left[q + \frac{p'}{\bar{\rho}} \right]$, $b = \frac{p'+q'\bar{\rho}}{p'+q'}$ and $A(n_0, n_1)$ remains to be determined. Inserting Eq. (7) in Eq. (1) yields

$$A(n_0 - 1, n_1) - \frac{n_0}{n_0 + n_1} A(n_0, n_1) = 0, \quad (8)$$

for $n_0, n_1 > 0$ with $A \equiv A(n_0, 0) = A(0, n_1)$ set by the normalization of P_{n_0, n_1} . This recursion relation is easily solved, giving

$$P_{n_0, n_1} = (1 - a - b) \binom{n_0 + n_1}{n_0} a^{n_0} b^{n_1}. \quad (9)$$

Having found the distribution of holes n_0 and bath particles n_1 between the tracers, we finally carry out the last step of our analysis. Taking a partial sum of P_{n_0, n_1} while keeping the distance between the two tracers $k \equiv n_0 + n_1$ fixed yields

$$Q(k) \equiv \sum_{n_0+n_1=k} P_{n_0, n_1} = (1 - a - b)(a + b)^k. \quad (10)$$

The fact that $Q(k)$ is exponentially decaying with the distance between the tracers may be attributed to an emergent strongly attractive linear potential $V(k) = -\ln(a+b)k$. It results in a two-tracer bound state whose average distance is $\langle k \rangle = (a+b)/(1-a-b) \ll 1$. Equation (10) clearly relates the bath density profile near the tracers, which enters via a and b , to their emergent attractive interactions and resulting condensation. In Fig. 3 we present a comparison of the MF expression for $Q(k)$ and numerical simulation results, showing a very good agreement.

Having analytically related the attraction and condensation of multiple driven tracers to the surrounding bath density in the 1D lattice model, we next validate this understanding in a far more realistic model. Consider a gas of elastic hard Brownian disks, of unit diameter and mass, confined to a 2D channel oriented parallel to the x axis. The channel is periodic along \hat{x} , with period L_x , and its width $L_y = 2 + \varepsilon$ is fixed by two thermal walls. We are interested in the case of $\varepsilon > 0$, where the channel is wide enough to allow the disks to overtake each other. The channel contains N bath disks of mean density $\bar{\rho} = N/(L_x L_y)$ and M tracer disks that are subjected to a constant force $\mathbf{F} = F\hat{x}$.

A typical configuration of the system is illustrated at

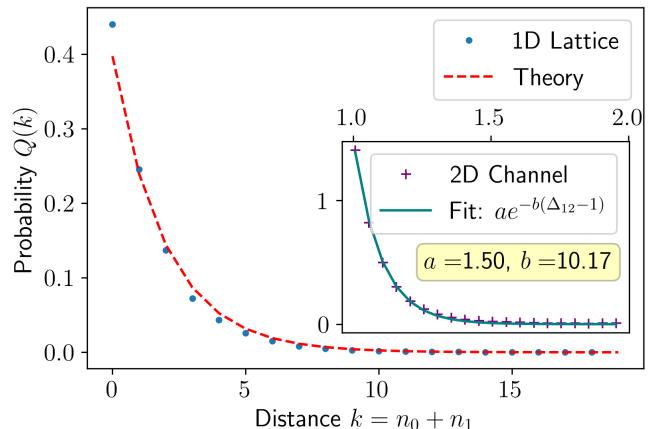


Figure 3. Histogram of the distance $k = n_0 + n_1$ between the two tracers in a 1D lattice of $L = 4096$ sites with a mean bath density of $\bar{\rho} = 0.2$ and rates $p = 1$ and $q = p' = q' = 0.001$. Inset: Analogous histogram for the distance Δ_{12} between two hard-core Brownian disk tracers in a 2D narrow channel of width $L_y = 2.1$ and length $L_x = 190$. The driving force is $F = 16$ and the mean bath particle density is $\bar{\rho} = 0.5$.

the bottom of Fig. 2. The particles evolve according to under-damped Langevin dynamics as is outlined in more detail in [41].

This model is numerically shown to exhibit the same characteristic features as in the lattice model's "localized" phase: a driven disk propagates at a finite velocity, even for large L_x , and generates a local disturbance to the bath density around it (see [41]). In addition, the model exhibits attraction and condensation when multiple tracer disks are simultaneously driven along the channel, as demonstrated in Fig. 1. Note that this robust emergent attraction occurs even though there are no direct attractive interactions between the tracers, and is observed to persist for a broad range of mean bath density and temperatures, as long as the channel is narrow enough and the drive is strong. No such attraction is observed for broad channels or weak drive. The inset of Fig. 3 shows the distribution function of the distance between two mutually bound tracers. As in the discrete lattice model, it is found to decay exponentially with the distance, here given by $\Delta_{12} - 1$ for disks of unit diameter, indicating an effective linear attractive potential. More details are provided in [41].

Acknowledgments - We thank Bertrand Lacroix-Achez-Toine for helpful discussions. This work was supported by a research grant from the Center of Scientific Excellence at the Weizmann Institute of Science. The generous allocation of computer resources at the VSC3 cluster operated by Austrian Universities is gratefully acknowledged.

-
- [1] Ekaterina M Nestorovich, Christophe Danelon, Mathias Winterhalter, and Sergey M Bezrukov. Designed to penetrate: time-resolved interaction of single antibiotic molecules with bacterial pores. *Proceedings of the National Academy of Sciences*, 99(15):9789–9794, 2002.
- [2] Michael P Rout, John D Aitchison, Marcelo O Magnasco, and Brian T Chait. Virtual gating and nuclear transport: the hole picture. *Trends in cell biology*, 13(12):622–628, 2003.
- [3] Michael A Welte. Bidirectional transport along microtubules. *Current biology*, 14(13):R525–R537, 2004.
- [4] Susan R Wenthe and Michael P Rout. The nuclear pore complex and nuclear transport. *Cold Spring Harbor perspectives in biology*, 2(10):a000562, 2010.
- [5] Greg Kabachinski and Thomas U Schwartz. The nuclear pore complex—structure and function at a glance. *J Cell Sci*, 128(3):423–429, 2015.
- [6] Marco Polin, Yohai Roichman, and David G Grier. Autocalibrated colloidal interaction measurements with extended optical traps. *Physical Review E*, 77(5):051401, 2008.
- [7] Christof Gutsche, Friedrich Kremer, Matthias Krüger, Markus Rauscher, Rudolf Weeber, and Jens Harting. Colloids dragged through a polymer solution: Experiment, theory, and simulation. *The Journal of chemical physics*, 129(8):084902, 2008.
- [8] Matthias Krüger and Markus Rauscher. Diffusion of a sphere in a dilute solution of polymer coils. *The Journal of chemical physics*, 131(9):094902, 2009.
- [9] I. Gazuz, A. M. Puertas, Th. Voigtmann, and M. Fuchs. Active and nonlinear microrheology in dense colloidal suspensions. *Phys. Rev. Lett.*, 102:248302, Jun 2009.
- [10] Raphaël Candelier and Olivier Dauchot. Journey of an intruder through the fluidization and jamming transitions of a dense granular media. *Physical Review E*, 81(1):011304, 2010.
- [11] Roel PA Dullens and Clemens Bechinger. Shear thinning and local melting of colloidal crystals. *Physical review letters*, 107(13):138301, 2011.
- [12] D. Winter, J. Horbach, P. Virnau, and K. Binder. Active nonlinear microrheology in a glass-forming yukawa fluid. *Phys. Rev. Lett.*, 108:028303, Jan 2012.
- [13] I. Gazuz and M. Fuchs. Nonlinear microrheology of dense colloidal suspensions: A mode-coupling theory. *Phys. Rev. E*, 87:032304, Mar 2013.
- [14] M. Gruber, G. C. Abade, A. M. Puertas, and M. Fuchs. Active microrheology in a colloidal glass. *Phys. Rev. E*, 94:042602, Oct 2016.
- [15] Todd M. Squires and John F. Brady. A simple paradigm for active and nonlinear microrheology. *Physics of Fluids*, 17(7):073101, 2005.
- [16] D. Mizuno, D. A. Head, F. C. MacKintosh, and C. F. Schmidt. Active and passive microrheology in equilibrium and nonequilibrium systems. *Macromolecules*, 41(19):7194–7202, 2008.
- [17] Todd M. Squires and Thomas G. Mason. Fluid mechanics of microrheology. *Annual Review of Fluid Mechanics*, 42(1):413–438, 2010.
- [18] Laurence G Wilson and Wilson CK Poon. Small-world rheology: an introduction to probe-based active microrheology. *Physical Chemistry Chemical Physics*, 13(22):10617–10630, 2011.
- [19] Brian J Kirby. *Micro-and nanoscale fluid mechanics: transport in microfluidic devices*. Cambridge university press, 2010.
- [20] Zhifeng Zhang, Jie Xu, and Corina Drapaca. Particle squeezing in narrow confinements. *Microfluidics and Nanofluidics*, 22(10):120, 2018.
- [21] SF Burlatsky, GS Oshanin, AV Mogutov, and M Moreau. Directed walk in a one-dimensional lattice gas. *Physics Letters A*, 166(3-4):230–234, 1992.
- [22] SF Burlatsky, G Oshanin, M Moreau, and WP Reinhardt. Motion of a driven tracer particle in a one-dimensional symmetric lattice gas. *Physical Review E*, 54(4):3165, 1996.
- [23] J De Coninck, G Oshanin, and M Moreau. Dynamics of a driven probe molecule in a liquid monolayer. *EPL (Europhysics Letters)*, 38(7):527, 1997.
- [24] C Landim, S Olla, and SB Volchan. Driven tracer particle in one dimensional symmetric simple exclusion. *Communications in mathematical physics*, 192(2):287–307, 1998.
- [25] O Bénichou, AM Cazabat, A Lemarchand, M Moreau, and G Oshanin. Biased diffusion in a one-dimensional adsorbed monolayer. *Journal of statistical physics*, 97(1-2):351–371, 1999.
- [26] P Illien, O Bénichou, C Mejía-Monasterio, G Oshanin, and R Voituriez. Active transport in dense diffusive single-file systems. *Physical review letters*, 111(3):038102, 2013.
- [27] Pierre Illien, Olivier Bénichou, Gleb Oshanin, and Raphaël Voituriez. Velocity anomaly of a driven tracer in a confined crowded environment. *Phys. Rev. Lett.*, 113:030603, Jul 2014.
- [28] Julien Cividini, Anupam Kundu, Satya N Majumdar, and David Mukamel. Exact gap statistics for the random average process on a ring with a tracer. *Journal of Physics A: Mathematical and Theoretical*, 49(8):085002, 2016.
- [29] J Cividini, A Kundu, Satya N Majumdar, and D Mukamel. Correlation and fluctuation in a random average process on an infinite line with a driven tracer. *Journal of Statistical Mechanics: Theory and Experiment*, 2016(5):053212, 2016.
- [30] A Kundu and J Cividini. Exact correlations in a single-file system with a driven tracer. *EPL (Europhysics Letters)*, 115(5):54003, 2016.
- [31] Sebastian Leitmann and Thomas Franosch. Time-dependent fluctuations and superdiffusivity in the driven lattice lorentz gas. *Phys. Rev. Lett.*, 118:018001, Jan 2017.
- [32] Olivier Bénichou, Vincent Démery, and Alexis Poncet. Unbinding transition of probes in single-file systems.

- Physical review letters, 120(7):070601, 2018.
- [33] Asaf Miron, David Mukamel, and Harald A Posch. Phase transition in a 1d driven tracer model. Journal of Statistical Mechanics: Theory and Experiment, 2020(6):063216, jun 2020.
 - [34] Asaf Miron and David Mukamel. Driven tracer dynamics in a one dimensional quiescent bath. arXiv preprint arXiv:2007.08168, 2020.
 - [35] Carlos Mejía-Monasterio and Gleb Oshanin. Bias-and bath-mediated pairing of particles driven through a quiescent medium. Soft Matter, 7(3):993–1000, 2011.
 - [36] Oleg A Vasilyev, Olivier Bénichou, Carlos Mejía-Monasterio, Eric R Weeks, and Gleb Oshanin. Cooperative behavior of biased probes in crowded interacting systems. Soft Matter, 13(41):7617–7624, 2017.
 - [37] Alexis Poncet, Olivier Bénichou, Vincent Démery, and Gleb Oshanin. Bath-mediated interactions between driven tracers in dense single files. Phys. Rev. Research, 1:033089, Nov 2019.
 - [38] Ivan Lobaskin and Martin R Evans. Driven tracers in a one-dimensional periodic hard-core lattice gas. Journal of Statistical Mechanics: Theory and Experiment, 2020(5):053202, may 2020.
 - [39] R Kusters and C Storm. Dynamic phase separation of confined driven particles. Europhysics Letters, 118:58004, 2017
 - [40] Kirone Mallick, The exclusion process: A paradigm for non-equilibrium behavior Physica A, 418:17, 2015.
 - [41] Sm. SM, 2020.

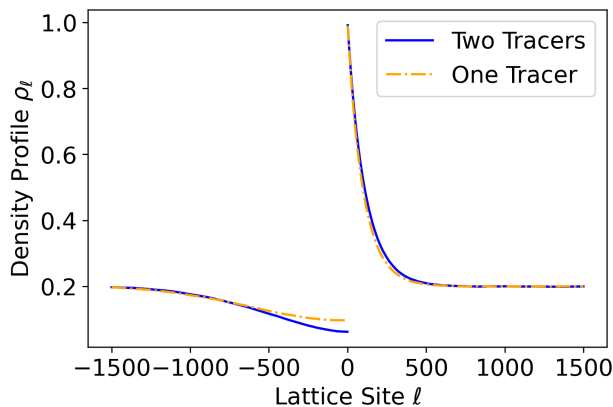


Figure S1. The stationary bath density profile ρ_ℓ in a lattice of $L = 4096$ sites at a distance of ± 1500 sites from the origin for a mean bath density of $\bar{\rho} = 0.2$ and rates $p = 1$ and $q = p' = q' = 0.001$. The solid blue curve shows the density profile of two driven tracers while the dashed orange curve shows the profile of a single driven tracer.

Supplemental Material

The 1D lattice model described in the main text was studied in [1] for a *single* driven tracer, where it was shown to feature two distinct phases: a “localized” phase, where the tracer attains a finite velocity and generates a localized deviation of the bath density from $\bar{\rho}$, and an “extended” phase, where the tracer’s velocity vanishes at large system length and the bath density profile extends across the entire system. In the main text, the attraction and condensation of multiple driven tracers is studied in the “localized phase”. This is done analytically for a 1D lattice SSEP model and numerically for a 2D channel model of hard-core driven Brownian disks. Here we provide support for two claims made in the main text: (1) the two-tracer bound state generates a bath density profile similar to the one generated by a *single* driven tracer and (2) for the case of two driven tracers, both the 1D lattice model and the 2D narrow channel exhibit the characteristic features of the single-tracer localized phase of Ref. [1] for the parameters considered in the main text.

I. NUMERICAL SIMULATIONS OF THE 1D LATTICE MODEL

Figure S1 presents the stationary bath density profile ρ_ℓ near the origin site $\ell = 0$ for one and two driven tracers. In the case of two driven tracers, the right (i.e. positive) part of the profile is provided in the rightmost

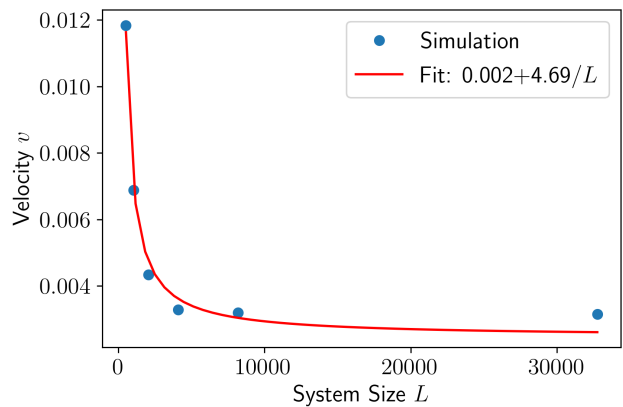


Figure S2. The stationary velocity v of the two-tracer bound pair versus system size L for a mean bath density of $\bar{\rho} = 0.2$ and rates $p = 1$ and $q = p' = q' = 0.001$. Blue dots denote direct simulation results while the solid red curve is a fit to $a + b/L$.

tracer’s (i.e. tracer 1) reference frame while the left (i.e. negative) part is provided in the leftmost tracer’s (i.e. tracer 2) frame. The figure shows close agreement of the density profiles near the tracers, supporting the understanding that the two-tracer bound state is well approximated by a single “effective” driven tracer.

The velocity of the two-tracer bound pair versus system size L is presented in Fig. S2. The figure clearly shows that a finite velocity is reached at large system sizes, as expected in the localized phase. Figure S3 shows a data collapse of the bath density profile for different system sizes. As expected in the localized phase, the deviation from $\bar{\rho}$ is indeed localized around the tracers and is independent of the system size L .

II. NUMERICAL SIMULATIONS OF THE 2D NARROW CHANNEL MODEL

In this section we elaborate on the 2D narrow channel model, discuss its numerical simulation scheme and present additional simulation results. The model consists of N bath disks and M externally driven “tracer” disks. The disks’ positions and velocities are respectively denoted by $\mathbf{r}_i = (x_i, y_i)$ and $\mathbf{v}_i = (v_{x,i}, v_{y,i})$, with $i = 1, \dots, N + M$. They evolve according to the Langevin dynamics

$$\dot{\mathbf{r}}_i = \mathbf{v}_i ; \quad \dot{\mathbf{v}}_i = -\gamma \mathbf{v}_i + \sqrt{2\gamma k_B T} \boldsymbol{\xi}_i + (\mathbf{F}) + \{\text{collisions}\}, \quad (11)$$

where γ denotes the friction coefficient, k_B the Boltzmann constant, and T the temperature. $\boldsymbol{\xi}_i(t)$ is

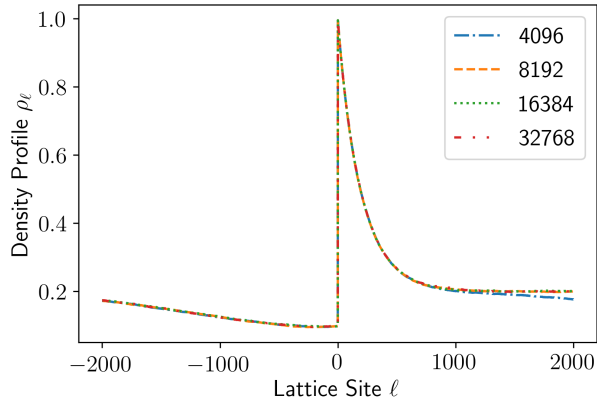


Figure S3. Data collapse of the stationary bath density profile ρ_ℓ for different system sizes L . The collapse focuses on the region near the bound two-tracer state. The mean bath density is $\bar{\rho} = 0.2$ and the rates are $p = 1$ and $q = p' = q' = 0.001$.

a Gaussian white noise satisfying $\langle \xi_i^\mu(t) \xi_j^\nu(t') \rangle = \delta_{ij} \delta^{\mu\nu} \delta(t - t')$, where δ_{ij} and $\delta^{\mu\nu}$ are Kronecker delta functions, $i, j = 1, 2, \dots, N + M$ denote particle indices, $\mu, \nu = 1, 2$ denote the two spatial directions, $\delta(t - t')$ is the Dirac delta function and the notation (\mathbf{F}) is used to indicate that the constant force $\mathbf{F} = F\hat{x}$ acts *only* on the tracers, not the bath disks. The last term in Eq. (11) encapsulates two kinds of collisions: elastic particle-particle collisions and "thermal" particle-wall collisions. In the latter case, the velocity components of the re-emitted disk parallel and perpendicular to the wall are drawn from two distinct distributions: Boltzmann distribution for the parallel component and a different distribution for the perpendicular one (See [2] for details). Reduced units are used, for which the particle diameter σ , its mass m , as well as k_B and T are all unity. In these units $\gamma = 2$ is used. The stochastic equations of motion are solved to first order in the time step according to the Gillespie updating scheme [3, 4].

We next demonstrate the qualitative similarities between the 1D lattice model and the 2D channel model. Unless noted otherwise, the following figures are obtained for parameters $F = 16$, $\bar{\rho} = 0.4$, $L_y = 2.6$ which we hereafter refer to as the "canonical" parameters.

Figure S4 displays the stationary average velocity $\langle v \rangle$ versus the channel length L_x for both a single driven tracer and a two-tracer bound state.

Figures S5 and S6 show the stationary density profile $n(r)$, respectively for a single driven tracer and a two-tracer bound state, for different values of N (and thus of L_x). As in the 1D lattice model, the profiles are plotted in the driven tracers' reference frame. The oscillations near the origin are a consequence of the crystal-

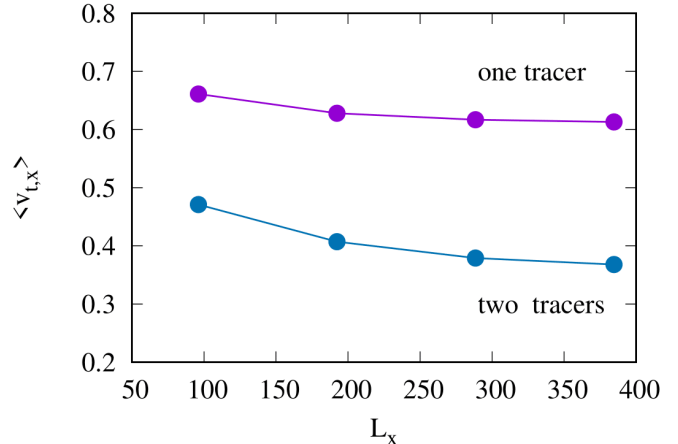


Figure S4. Stationary tracer velocity, $\langle v_{t,x} \rangle$, along the channel axis as a function of the channel length L_x for the narrow channel model. The solid lines are for guidance of the eyes. For the simulation the canonical parameters were used.

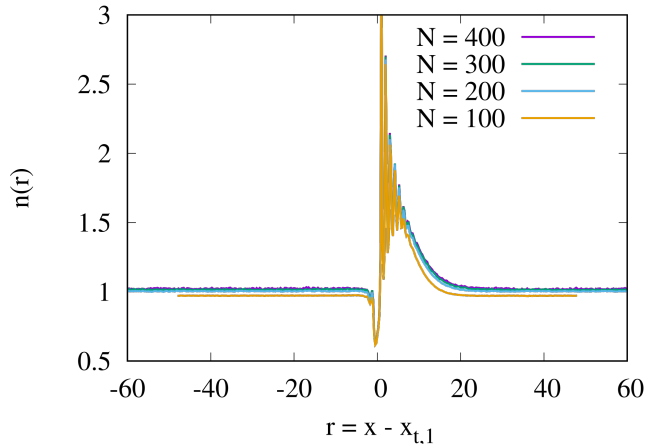


Figure S5. System size dependence of the density profile for the narrow channel containing a single tracer. A data collapse for profiles with various lengths L_x is observed for large systems.

like spatial arrangement of the dense bath particles that accumulated in front of the tracer(s). This high density region is analogous to that appearing in Fig. S3 for the 1D lattice model, as well as the evident data collapse which becomes more pronounced as L_x increases.

Figure S7 shows a plot the distance along the x direction between the two driven tracers $\Delta_{1,2}$ versus time. Two different values of the driving force are considered for a channel of width $L_y = 2.1$ with a mean bath density $\bar{\rho} = 0.5$. In the top figure, obtained for $F = 8$,

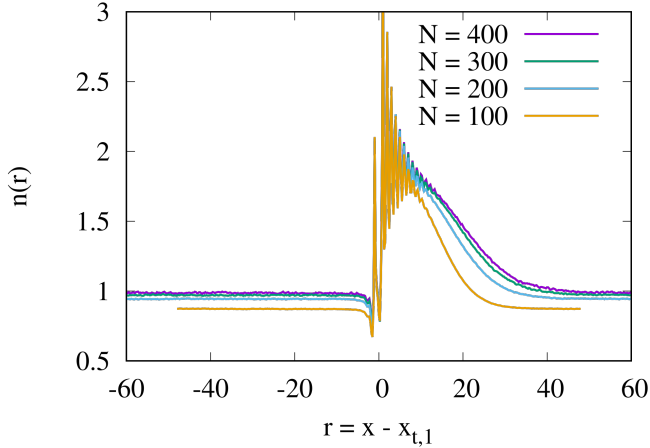


Figure S6. System size dependence of the density profile for the narrow channel model containing two tracers. A data collapse for profiles with various lengths L_x is observed for large systems.

the distance is shown to remain very small at all times,

roughly of $\mathcal{O}(1)$, irrespective of the channel's length L_x . The bottom figure, obtained for $F = 4$, demonstrates that this typical distance grows as the driving force is weakened. Further reducing F beyond some critical value, or equivalently increasing the channel width L_y at fixed F , breaks the tracers' bound state. Nevertheless, this bound state persists for a range of F and L_y .

Figure S8 shows the distribution of distances $\Delta_{1,2}$ in the stationary state. The central domain of P , $-1 < \Delta_{12} < 1$, corresponds to configurations where the two tracers lie one above the other in the channel where they are confined by the geometrical restrictions imposed by the channel. Their distance distribution in this domain is determined by the details of their mutual frequent collisions which need to be studied separately. On the other hand the two domains $1 < |\Delta_{12}| < 2$, which correspond to well separated tracers, do show an exponential behavior, which qualitatively agrees with the exponential behavior of the probability distribution $P(k)$ obtained for the 1D lattice model in Fig. 3 of the main text.

-
- [1] Asaf Miron, David Mukamel, and Harald A Posch. Phase transition in a 1d driven tracer model. Journal of Statistical Mechanics: Theory and Experiment, 2020(6):063216, jun 2020.
- [2] Riina Tehver, Flavio Toigo, Joel Koplik, and Jayanth R. Banavar. Thermal walls in computer simulations. Phys.

- Rev. E, 57:R17–R20, Jan 1998.
- [3] Daniel T Gillespie. Exact numerical simulation of the Ornstein-Uhlenbeck process and its integral. Physical review E, 54(2), 2084, 1996.
- [4] Daniel T Gillespie. The mathematics of Brownian motion and Johnson noise. American Journal of Physics, 64(3), 225-240, 1996.

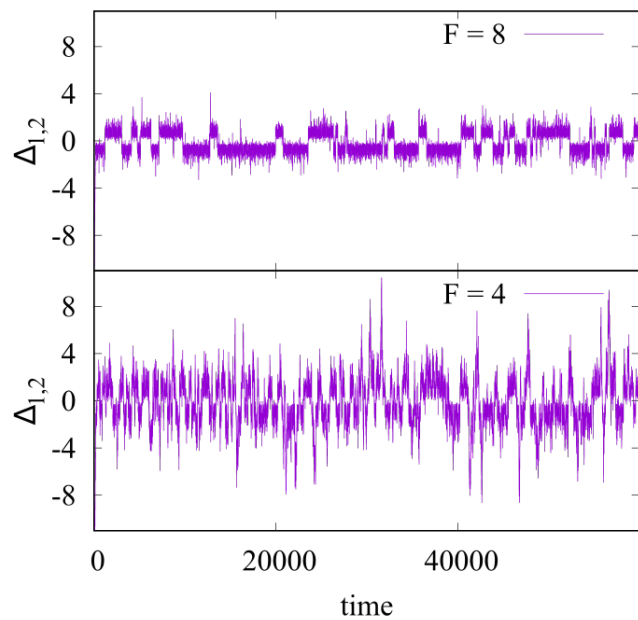


Figure S7. Separation of the two tracers in a narrow channel of width $L_y = 2.1$ as a function of time. Top: $F = 8$. This field is strong enough to prevent the particle pair from separating. Bottom: $F = 4$. This value is close to the separation threshold of the two tracers. The other parameters are $\bar{\rho} = 0.5$ and $L_x = 190.5$.

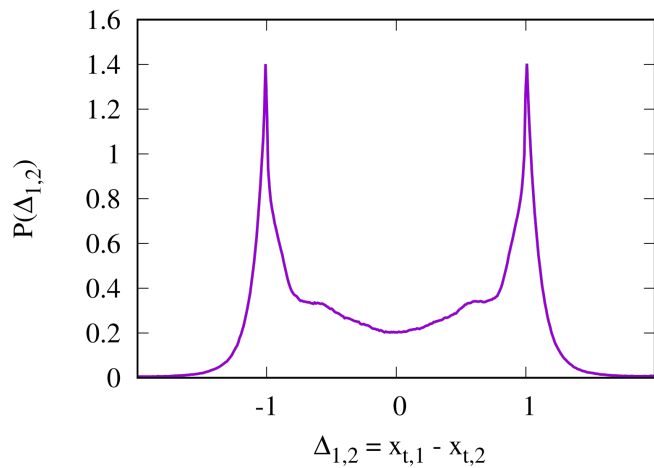


Figure S8. Probability distribution of the tracer separation in x direction, $\Delta_{1,2} = x_{t,1} - x_{t,2}$, for two bound tracers in a narrow channel of length $L_x = 96.2$.